INT. J. NUM. METH. HEAT FLUID FLOW, VOL. 6 NO. 4, 3–24 (1996)

A FINITE VOLUME METHOD FOR THE SOLUTION OF CONVECTION-DIFFUSION 2D PROBLEMS BY A QUADRATIC PROFILE WITH SMOOTHING

L. DE BIASE†, F. FERAUDI† AND V. PENNATI‡

†*University of Milano, Department of Mathematics, Via C. Saldini 50, 20133 MILANO, Italy*
‡*ENEL SpA-CRIS, Via Ornato 90/14, 20162 MILANO, Italy*

ABSTRACT

A new finite volume (FV) method is proposed for the solution of convection-diffusion equations defined on 2D convex domains of general shape. The domain is approximated by a polygonal region; a structured non-uniform mesh is defined; the domain is partitioned in control volumes. The conservative form of the problem is solved by imposing the law to be verified on each control volume. The dependent variable is approximated to the second order by means of a quadratic profile. When, for the hyperbolic equation, discontinuities are present, or when the gradient of the solution is very high, a cubic profile is defined in such a way that it enjoys unidirectional monotonicity. Numerical results are given.

KEY WORDS Convection Diffusion Finite volume

INTRODUCTION

In some of our preceding work we described several 1D techniques for the FV solution of convection-diffusion problems, based on the use of a profile for the dependent variable, which did not need the volumes to be equal and which, by the study of the normalized variable diagram (NVD), yielded intrinsically monotonic behaviour[1].

In that paper we showed how a weighted ν-splines approximation of the local behaviour of the unknown physical variable can yield a very accurate treatment of the problem.

We are not proposing a 2D version of that method here; actually, although we believe such an extension could be extremely effective, we are trying to build a very simple profile (quadratic on most of the domain), which provides a very interesting point of view and which will be of value in comparison with any other results. The main points on which we are focusing are an adaptive definition of volumes, a smoothing technique for the regions where oscillations are detected and an accurate approximation of boundary conditions on polygonal regions.

The main advantages of the method we are presenting are the third order of approximation of the convective term on uniform 1D grids (the second on 1D and 2D non-uniform grids, with significant differences in volume sizes) and a cell-centre approach, which seems to be the best choice for incompressible fluids[2] (and this is of relevance to us since we work on the solution of Navier-Stokes' equation).

Several FV methods have been proposed in the literature for convection-diffusion problems, and some of them are rather effective[3].

For most of the FV methods based on a structured domain discretization, with a finite difference approximation of the physical variables, it is compulsory to work on rectangular regions with a uniform subdivision, i.e. with all the volumes identical rectangles.

0961–5539

Received August 1994
Revised January 1996

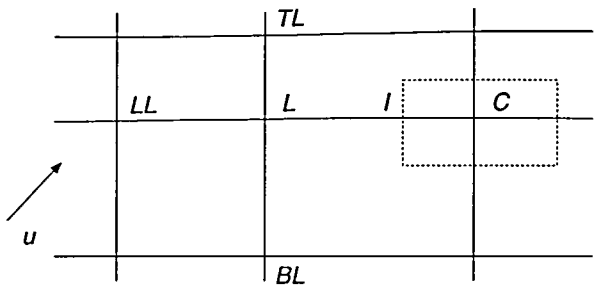

Figure 1 Points that can be included when working on the volume centred at *C*

Since obviously not all real-world problems are defined on rectangles, two are the typical choices for their solution: a transformation of the physical domain into a computational rectangle[4] or the solution on the domain as given, by means of not necessarily equisized or equishaped volumes. We chose the second alternative, which is much more flexible and yet it can easily be implemented, thanks to the good approximation of boundary conditions.

The basic idea of our method is rather similar to that inspiring QUICK[5], where a weighted quadratic interpolation is used for the local approximation of the convective term (while the diffusive part is approximated by centred differences). In QUICK the behaviour of the convective term on a face of a given volume (in 2D) is obtained on the basis of five proper nodes of a structured regular mesh. The choice of nodes depends on the velocity direction, in order for the approximation to exhibit an upwind character.

If the velocity components u_l and v_l are positive, the points involved in the approximation of the dependent variable ϕ_l on face l are as in *Figure 1* and the value for ϕ_l is

$$\phi_l = \frac{1}{2}(\phi_C + \phi_L) - \frac{1}{8}(\phi_C - 2\phi_L + \phi_{LL}) + \frac{1}{24}(\phi_{TL} - 2\phi_L + \phi_{BL}). \tag{1}$$

With respect to boundary conditions, QUICK works as in one dimension, i.e. some external fictitious points are introduced and the profile is used also at boundary volumes. The order of approximation of the method is the second[6]. In our method, as will be clear in next section, the interior of the domain is discretized by means of a structured grid, not necessarily uniform, so that the internal volumes are rectangles, and not necessarily equal. The volumes close to the boundaries can be of different shapes and sizes, depending on the domain of definition. This implies that, where the solution requires a more accurate study, a refined grid can be used.

OUR METHOD: 1D VERSION

Consider the 1D convection diffusion equation

$$\frac{\partial \rho\phi}{\partial t} = -\frac{\partial \rho u\phi}{\partial x} + \frac{\partial}{\partial x}\left(\Gamma \frac{\partial \phi}{\partial x}\right) + Q \tag{2}$$

defined on domain Ω, of boundary S, where ϕ is the dependent variable, $u(x, t)$ the convective velocity, ρ the density, Γ the diffusion coefficient and Q the source term.

Its conservative form is

$$\frac{\partial}{\partial t}\int \rho\phi \, d\Omega + \oint_S (\rho u\phi - \Gamma \nabla\phi) \, dS = \int_\Omega Q \, d\Omega. \tag{3}$$

After Ω has been divided in n subdomains Ω_i, such that $\check{\imath}\, \Omega_i = \Omega$, we impose the equation to be verified on each Ω_i. In subdividing Ω we do not require the volumes to be equal (see *Figure 2*).

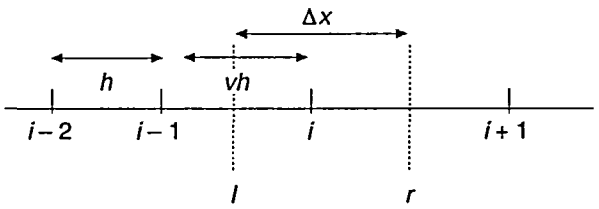

Figure 2 1D division in unequal volumes

We define a grid of points on Ω and put the volume faces at mid-distance between any two consecutive nodes. Integration of (3) in space on a volume of amplitude Δx and in time between t and $t + \Delta t$ with an explicit method yields

$$\rho_i \phi_i^{n+1} = \rho_i \phi_i^n + (\rho_l c_l \phi_l - \rho_r c_r \phi_r)^n + \left(\alpha_r \left.\frac{\partial \phi}{\partial x}\right|_r - \alpha_l \left.\frac{\partial \phi}{\partial x}\right|_l \right)^n \Delta x + Q \Delta t \tag{4}$$

where:

the apex $n + 1$ refers to time instant $t + \Delta t$,

the apex n to time instant t,

$c_f = u\Delta t/\Delta x$ is the local Courant number ($f = l$ or $f = r$),

$\alpha_f = \Gamma \Delta t/\Delta x^2$ is the local diffusion parameter,

Q is the space-time average of the source term.

Consider u_l, the convective velocity on the left face of a given volume, to be positive; if this is not the case, all is equally applied by the reverse node ordering. With the assumption of positive velocity we define for face l of the control volume of *Figure 2* a quadratic profile interpolating the unknown solution at nodes $i - 2$, $i - 1$, i (2 in the upstream direction, 1 in the downstream one). If the amplitudes of intervals $[i - 2, i - 1]$ and $[i - 1, i]$ are h and vh respectively, the expression of our profile on the left face of the volume is,

$$\phi_l = -\frac{v^2}{4(v+1)} \phi_{i-2} + \frac{v+2}{4} \phi_{i-1} + \frac{v+2}{4(v+1)} \phi_i \tag{5}$$

Obviously, if $v = 1$, i.e. if the involved intervals are equal, profile (5) reduces to QUICK.

Although the volumes are not equal, for a C^3 solution this profile yields a truncation error of

$$\frac{v^2 h^3 (v+2)}{48} \phi_l'''$$

i.e. it provides a third order approximation. For the diffusive part (if any) centred differences are used, so that the order of approximation of the method for solving (3) reduces to the second.

The approximation of boundary conditions can be performed in several ways: if Dirichlet conditions are given, their value is used at the boundary point (i.e. the boundary face of the first/last volume), while the derivative can be approximated by centred differences if an external fictitious point is introduced. Otherwise generalized finite difference formulae (GFDF) of the desired order[7], based on a completely asymmetric stencil, can be used, both for the aforementioned situation and for the case when boundary conditions involving the normal derivative are given. With the second choice, the order of approximation can be as high as wanted, but some computational cost has to be paid for the different treatment of boundary volumes.

For this reason, in the interior of the domain, our method is rather similar to QUICK, apart from the fact that, wherever the solution is smooth enough, a lower number of volumes can be used, thanks to the non-uniform mesh.

The main difference between the two methods is in the treatment of boundary conditions, which, in our method, are approximated with higher precision, i.e. by GFDF of third order, with

no external fictitious points. Actually in QUICK one or two external fictitious points are introduced for the approximation of the convective term on both faces of the first/last volume.

In our method, the non-uniform size of the volumes does not require the introduction of any fictitious point, since we can use the information given by boundary conditions by defining a boundary node on the boundary face of the first/last volume. For a wider description of the treatment of boundary conditions see the 2D version of our method in a subsequent section.

SMOOTHING

A problem connected with discontinuities ($\Gamma = 0$ in equation (3)) in the solution or with high gradients is the oscillatory behaviour the numerical solution can exhibit in many FV methods. Several interesting results were obtained to overcome this difficulty[8-10] and, among others, the study of NVD profiles[11]. NVD variables are very interesting because they allow defining sufficient conditions in order that profiles be monotonic, as in Sweby[12] to guarantee that the scheme enjoys the property of total variation diminishing.

In Leonard[11] monotonicity of some FV profiles (e.g. TVD) is considered: these profiles are extremely effective for some classes of problems, but they turn out to be inadequate for other types of benchmark problems. A normalization such as

$$\phi^* = \frac{\phi - \phi_U}{\phi_D - \phi_U}$$

(see *Figure 3*) produces the very interesting advantage that Φ^* does not depend on Φ_D and Φ_U (which become 1 and 0, respectively), so that its expression becomes much simpler. Besides simplicity, it was shown[6] that the third order of approximation and stability on equal volumes are ensured whenever the NVD profile includes point $Q = (1/2, 3/4)$, with derivatives at Q of 3/4.

If we work at our quadratic profile on unequal volumes, a generalized point

$$Q_1 = \left(0.5, \frac{(\nu+2)(\nu+3)}{8(\nu+1)}\right)$$

comes out and the derivative at it becomes $\nu + 2/4$. The third order still holds, as discussed above. By replacing $\nu = 1$, i.e. on equal volumes Q_1 reduced to Q and the derivative takes on value 3/4.

For the "critical" regions we are therefore looking for a profile verifying the following conditions:

$$\Phi^*(0) = 0, \Phi^*(1) = 1, \Phi^*(0.5) = \frac{(\nu+2)(\nu+3)}{8(\nu+1)} < 1, \Phi^{*\prime}(0.5) = \frac{\nu+2}{4}. \tag{6}$$

The simpler monotonic profile which can verify the above conditions is cubic and, for a face f in the unit square, it has the following expression:

$$\Phi_f^* = (2-\nu)(\phi_C^*)^3 + \frac{\nu^2 - 2\nu - 4}{\nu+1}(\phi_C^*)^2 + \frac{2\nu+3}{\nu+1}\phi_C^*. \tag{7}$$

By imposing $\Phi^*(0.5) < 1$ we obtain a condition on the ratio ν to ensure the order of approximation be maintained. Such a condition is

$$\nu \in [(3-\sqrt{17})/2, (3+\sqrt{17})/2] \tag{8}$$

which, in fact, we replace with the strictest condition

$$\nu \in [1/3, 3] \tag{9}$$

because of similarity reasons to those we obtained in[1].

Out of the unit square we use our quadratic profile (in NVD), a part for the immediate vicinity of the unit square itself, where linear profiles are used to connect ours to the origin, on the left, and to point (1, 1), on the right.

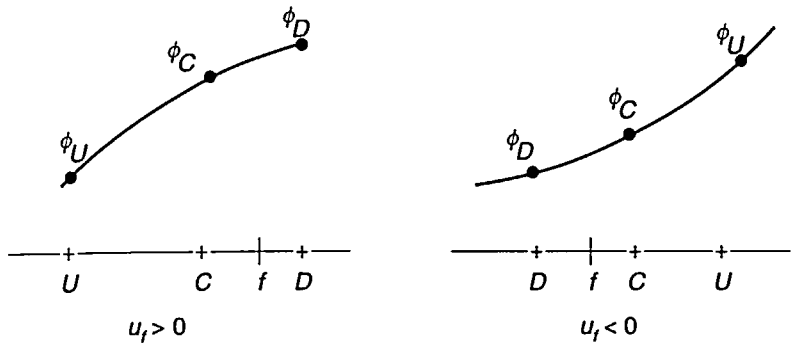

a) Stencils for positive and negative velocity

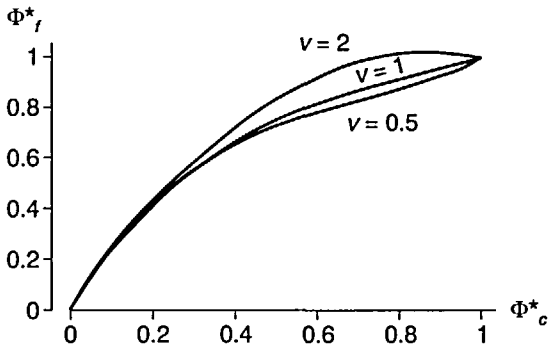

b) Cubic profiles in NVD for $v = 1$, $v = 0.5$ and $v = 2$

Figure 3

A similar strategy was introduced in Leonard and Mokhtari[13], to build a EULER-QUICK profile, which uses a combination of QUICK and Exponential Upwinding profiles in the unit square, and of upwind and centred differences approximations out of the unit square.

Comparison of numerical results of our method with those provided by EULER-QUICK on the classical benchmark problems[5] showed a high similarity, with a slightly higher numerical diffusion for our method, but with a significantly lower number of volumes and a lower computational cost. For a different strategy, which provides intrinsically monotonic profiles of third order, see Pennati *et al.*[1].

VON-NEUMANN STABILITY

For the 1D version of our method, with unequal volumes, we studied stability by applying the finite Fourier transform $\hat{\phi}_l$ of the numerical solution ϕ_i ($i = 0, 1, \ldots, M-1$, where M is the number of nodes) on a domain of amplitude L, for a pure convection equation, with an explicit temporal discretization, i.e. for the formulation

$$\phi_i^{n+1} = \phi_i^n - c_f\left(\frac{1}{8}\phi_{i-2}^n - \frac{v^2+3v+3}{4(v+1)}\phi_{i-1}^n + \frac{2v+1}{8}\phi_i^n + \frac{v+2}{4(v+1)}\phi_{i+1}^n\right). \qquad (10)$$

The Fourier transform is inverted, then it is applied to all the terms appearing in (10). By equating the corresponding coefficients we obtain

$$\hat{\Phi}_l^{n+1} = \hat{\Phi}_l^n \left\{\alpha \exp\left(-4\pi j\, x_l / L\right) + \beta \exp\left(-2\pi j\, x_l / L\right) + 1 + \gamma + \delta \exp\left(2\pi j\, x_l / L\right)\right\} \tag{11}$$

where

$$\alpha = -c_f/8, \beta = c_f \frac{\nu^2 + 3\nu + 3}{4(\nu+1)}, \gamma = -c_f \frac{2\nu+1}{8}, \delta = -c_f \frac{\nu+2}{4(\nu+1)},$$

x_l is the current abscissa and j is the imaginary unit.

In terms of the phase variable $\vartheta = 2\pi x_l/L$, the amplification factor[14,15]

$$G = \frac{\phi(x, t+\Delta t)}{\phi(x,t)}$$

is therefore

$$G = \alpha \exp(-2j\vartheta) + \beta \exp(-j\vartheta) + 1 + \gamma + \delta \exp(j\vartheta) \tag{12}$$

By the necessary and sufficient condition $|G| \le 1$, which ensures stability on an infinite domain, we obtain

$$c_f \le \frac{8(\cos^2\vartheta - (\nu+1)\cos\vartheta + \nu)}{(\cos^2\vartheta - (\nu+1)\cos\vartheta + \nu)^2 + \left(\frac{\nu^2+4\nu+5}{\nu+1} - \cos\vartheta\right)^2 \sin^2\vartheta} \tag{13}$$

which provides a stability region as in *Figure 4*.

A few comments on *Figure 4*: the values for ν (the ratio between amplitudes of two consecutive volumes were chosen in interval [1/3, 3], as discussed previously, although, in practice, refinements are performed by halving the amplitudes of volumes where needed. The plotted surface shows how the values of ν and ϑ (i.e. the relative volume sizes and the position in the domain) influence stability.

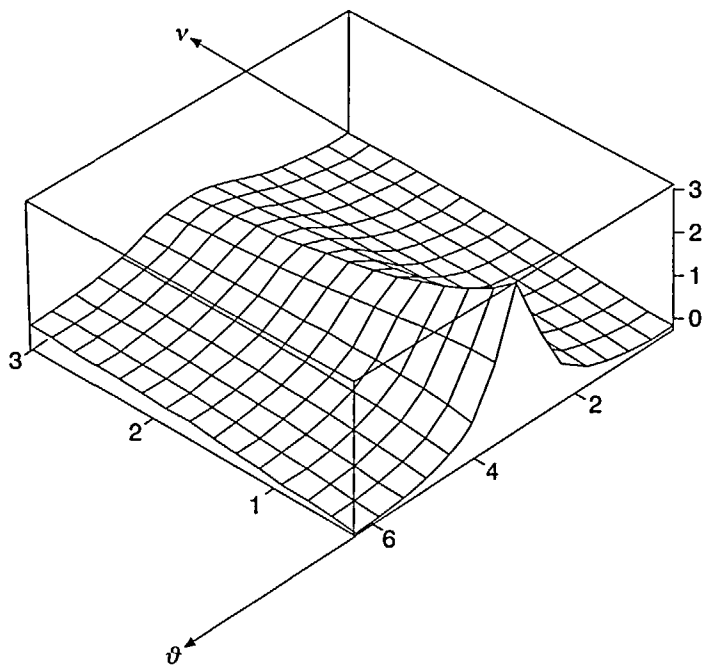

Figure 4 Stability region for the hyperbolic equation

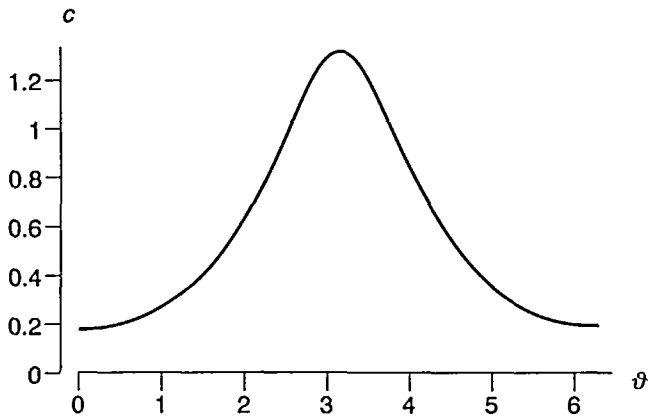

Figure 5 Section of *Figure 4*: stability region for $\nu = 2$

It can be seen that the strongest limitations correspond to $\vartheta = 0$ and $\vartheta = 2\pi$, whatever ν. We remark, however, that these values of ϑ represent the left and right boundaries of the domain respectively, where a different type of computation is adopted, so that these bounds do not in fact apply. Obviously, if refinements are actually performed in some region of the domain and if they imply halving the amplitude of some volume, the sections of the plotted surface to be considered in order to find the appropriate stability conditions are those relative to $\nu = 0.5$ and to $\nu = 2$, since, if some critical region is in the interior of the domain, the volume size is halved immediately before and doubled immediately after that region.

The stability region relative to $\nu = 2$ is shown in *Figure 5*. Bounds for Δt are the straightforward consequence of (13).

OUR METHOD: 2D VERSION

The 2D method we devised was inspired by some basic purposes: first of all we wanted to be able to deal with general shape domains without transforming them into computational rectangles; it was therefore essential for the volumes not to need equal shapes and sizes. Moreover, we wanted accurate profiles and a precise approximation of boundary conditions while we did not want oscillatory behaviours. We are going to describe the main steps of our method.

First of all, given a physical domain $\Omega \subset \mathbb{R}^2$ of general shape we define a polygonal approximation of its boundary[16]. Each side of the polygonal region is defined by its endpoints and for each vertex incidence information is recorded. For each side (or piece of side) the type of given boundary conditions is identified. Subsequently a structured non-uniform mesh is defined in such a way that no grid line crosses vertices of the polygonal region. The volumes are built by putting their faces on the boundary or at mid-distance between any two consecutive grid lines.

For boundary volumes, whenever a situation such as that in *Figure 6* occurred, we introduced inclined sides as in *Figure 7*, so that a volume face is always in common to exactly two volumes (actually, when this is not the case, conservation could be lost).

The problem to be solved, in 2D, is

$$\frac{\partial}{\partial t}\int_\Omega \rho\phi \, d\Omega + \oint_S F \, dS = \int_\Omega Q_V \, d\Omega + \oint_S Q_S \, dS \tag{14}$$

which, in discrete form becomes

$$(\phi_i^{n+1} - \phi_i^n) A_i + \Delta t \sum_{sides} (F_C + F_D) \cdot L_i = \Delta t \sum_{sides} Q_S L_i + \Delta t \, Q_V A_i \tag{15}$$

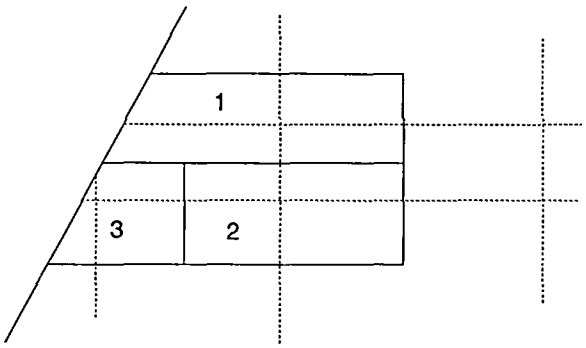

Figure 6 Volume 1 has a face in common with both volumes 2 and 3

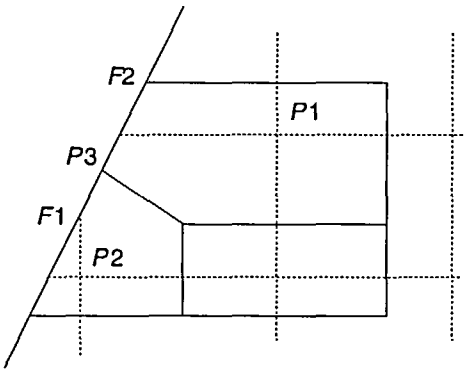

Figure 7 New subdivision which ensures numerical conservation

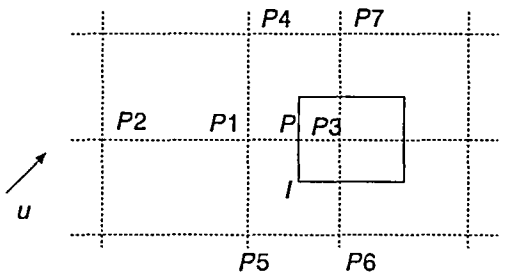

Figure 8 Points that can be involved when working on the volume centred at $P3$

where A_i are the volume areas, L_i are the oriented lengths of its faces, Q_S and Q_V are the surface and volume sources, respectively (the sum is over all the sides of the control volume CV), F_C and F_D are the convective and diffusive fluxes, integrated on volume sides.

As already done in 1D, we defined a quadratic profile in two variables and kept the upwind philosophy for the choice of the interpolation points. If, for instance, for the control volume of *Figure 8*, we assume the velocity components u_x and u_y to be positive, for face l of the control volume our profile turns out to be

$$\phi_l = A\phi_{P1} + B\phi_{P2} + C\phi_{P3} + D\phi_{P4} + E\phi_{P5} + F\phi_{P6} \tag{16}$$

where coefficients A, B, C, D, E, F are combinations of the co-ordinates of points $P1, P2, P3, P4, P5, P6$ and of the physical volume dimension:

$$A = \frac{3b(q-s)+3c(s-q)-2(q+s)^2}{24ab} + \frac{s-q}{8b} + \frac{k}{2(k-h)}$$

$$B = \frac{k^2}{(h+k)(h-k)} + 1$$

$$C = \frac{q-s}{8s} + \frac{k}{2(h+k)} \tag{17}$$

$$D = \frac{3(b-c)(q-s)-2(q+s)^2}{24b(a+b)} + \frac{3c(q-s)+2(q+s)^2}{24ab} - \frac{q-s}{8a}$$

$$E = \frac{q-s}{8b} - \frac{3(b-c)(q-s)-2(q+s)^2}{24b(a+b)}$$

$$F = -\frac{q-s}{8c}$$

where the above co-ordinates are defined with respect to a local co-ordinate system with origin at P, so that $P1 = (-h, 0)$, $P2 = (-k, 0)$, $P3 = (h, 0)$, $P4 = (-h, a)$, $P5 = (-h, -b)$, $P6 = (h, -c)$, with $h = dk$, q is the half distance between $P7$ and $P3$ and s is the half distance between $P6$ and $P3$.

For smooth enough solutions, this profile yields a second order approximation, (the third in the x direction) as can easily be verified by Taylor series expansion.

For boundary volumes we decided, whenever possible, to keep a uniform strategy of treatment as for internal volumes: this implied, for the approximation of the diffusive term, the introduction of some external fictitious points, which could subsequently be eliminated by means of boundary conditions. When a little additional computational cost is accepted and the order of approximation is of relevance, the diffusive term is approximated by asymmetric GFDF, without defining external fictitious points.

When inclined sides have to be introduced between two volumes (V_1 and V_2 of *Figure 7*, say), if we have Dirichlet boundary conditions, we approximate the convective term by the average of values at points P_1, P_2, F_1 and F_2, while the value of the diffusive term on the inclined side is set to the value at P_3 or to the average of values at F_1 and F_2; if boundary conditions are of Neumann type, the normal derivative on the inclined side is attributed the value it takes on at P_3.

Obviously, this is not the only possible choice, but our first aim here was simplicity and low computational cost, more than the local order of approximation.

For the approximation of derivatives of the unknown solution we adopted centred differences or GFDF, depending on the position of the volume face at study.

BOUNDARY CONDITIONS

We are now going to describe how our method acts with respect to the classical types of boundary conditions.

If boundary conditions are of INFLOW type, they can assign the value of the dependent variable or both the values of the normal derivative and of the dependent variable at the boundary.

When both values are available, convective and diffusive terms are directly integrated on the boundary faces; moreover, the value of ϕ at the boundary nodes can be used in the approximation relative to the internal faces of the same volume.

When, on the contrary, no information on the normal derivative is given, if a diffusive term is present, an external fictitious point is introduced or asymmetric GFDF are used (see Appendix). The value of the dependent variable at such an external point is computed by quadratic

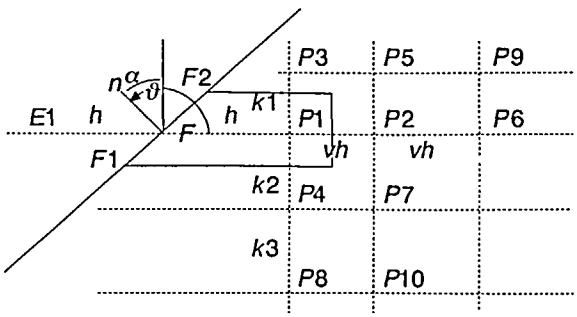

Figure 9 Points that can be involved when working on the boundary of the volume centred at $P1$

extrapolation, obtained by means of the 1D profile (5), with the obvious changes in node names. The value of the normal derivative at point F is approximated to second order by means of GFDF involving points $P1$, $P2$, $P3$, $P4$, $P5$ and $E1$ (*Figure 9*).

If we are assigned NOFLOW boundary conditions, the velocity field is null at the boundary and the convective term vanishes.

If the value of the normal derivative is given, the value of ϕ at the boundary node is determined by GFDF of third order (with no external point). If the value of ϕ at the boundary is given, GFDF of second order (with no external point) are used for the approximation of the normal derivative at F (*Figure 9*).

Finally, if OUTFLOW boundary conditions are given, the standard choice is to assume null gradient or null curvature at the boundary. We adopted the first choice and approximated the dependent variable ϕ by imposing $\partial\phi/\partial n = 0$ at the boundary node F by means of GFDF.

We remark that the approximation of ϕ, or of its normal derivative, by means of GFDF at the boundary of general shaped domains can be obtained, at the desired order of approximation, by proper Taylor expansions and no external fictitious points need be introduced[16].

SMOOTHING OF THE SOLUTION

At the first time instant, a numerical solution is obtained by means of our quadratic profile. If some oscillations are detected, a smoothing procedure is adopted. Such procedure is now described for face l of the control volume in *Figure 8*. The smoothing technique is repeated, with obvious changes, for all of the faces of the control volume; its aim is the imposition of monotonicity, on each volume face, along the direction orthogonal to the face itself. For the left face of the volume (*Figure 8*) our profile is

$$\phi_l = \frac{1}{2}(\phi_{P1} + \phi_{P3}) - \frac{2h}{4(k-h)(k+h)}(2h\phi_{P2} - (h+k)\phi_{P1} + (k-h)\phi_{P3}) + \\ + R_1\phi_{P1} + R_2\phi_{P3} + D\phi_{P4} + E\phi_{P5} + F\phi_{P6} \tag{18}$$

where we can single out a linear contribution

$$\phi_{lin} = (\phi_{P1} + \phi_{P3})/2, \tag{19}$$

a term we can name "normal curvature"

$$n\text{curv} = \frac{2h}{4(k-h)(k+h)}(2h\phi_{P2} - (h+k)\phi_{P1} + (k-h)\phi_{P3}), \tag{20}$$

and a term which, for equisized volumes, represents a transverse curvature, so that, by extension, we shall again name "transverse curvature"

$$t\text{curv} = R_1\phi_{P1} + R_2\phi_{P3} + D\phi_{P4} + E\phi_{P5} + F\phi_{P6}. \tag{21}$$

Therefore our profile is composed by a unidirectional contribution (19), (20), which equals the 1D profile (5) and by a term (21), giving the contribution of the second dimension.

For the sake of simplicity we worked at the 2D shape preserving by considering monotonicity with respect to the direction orthogonal to the volume face at study.

In order, e.g. to impose monotonicity with respect to variable x, on the face l of *Figure 8*, it is sufficient to replace the first two terms by the cubic profile described earlier, or its extensions out of the unit square. The resulting profile is therefore

$$\phi_l = \phi_{P2} + (\phi_P - \phi_{P2})\,\phi_l^* + R_1\phi_{P1} + R_2\phi_{P3} + D\phi_{P4} + E\phi_{P5} + F\phi_{P6} \tag{22}$$

where, by setting $v = 2h/(k-h)$, we have:

$$\phi_l^* = (2-v)\,(\phi_{P1}^*)^3 + \frac{v^2 - 2v - 4}{v+1}(\phi_{P1}^*)^2 + \frac{2v+3}{v+1}\phi_{P1}^*, \tag{23}$$

where Φ^* is the NVD transformed variable and $P2$ and $P3$ are the upstream and downstream nodes, respectively.

At the subsequent time instants, depending on the a priori knowledge we have on the solution, we can adopt a predictor-corrector attitude, by which the quadratic profile is used and replaced by the cubic one in the regions of high gradient.

NUMERICAL EXAMPLES IN 1D

In order to test the performance of our method, we solved an advection unsteady 1D equation:

$$\frac{\partial \Phi}{\partial t} + u\frac{\partial \Phi}{\partial x} = 0 \tag{24}$$

on interval [0, 1], with inflow boundary conditions $\phi(0) = 1$. Its analytical solution is

$$\Phi(x,t) = \begin{cases} 1 & 0 \le x \le 0.2 + t \\ 0 & x > 0.2 + t \end{cases} \tag{25}$$

The comparison between our results (represented by a series of dots) and the analytical solution (represented by the continuous line) and that between an upwind scheme and the analytical solution are shown in *Figure 10*.

A parabolic stationary equation was also solved[13]:

$$u\frac{\partial \Phi}{\partial x} = \Gamma\frac{\partial^2 \Phi}{\partial x^2} + S(x) \tag{26}$$

with

$$S(x) = \begin{cases} 10 - 50x & 0 \le x \le 0.3 \\ 50x - 20 & 0.3 < x \le 0.4 \\ 0 & 0.4 < x \le 1 \end{cases} \tag{27}$$

In *Figure 11* the centred solution, the QUICK solution and our solution are represented.

NUMERICAL EXAMPLES IN 2D

In order to test effectiveness of our method we solved some 2D problems.

Problem 1: the stationary equation

$$u\frac{\partial \phi}{\partial x} + v\frac{\partial \phi}{\partial y} = \frac{\partial^2 \phi}{\partial x^2} + \frac{\partial^2 \phi}{\partial y^2} \tag{28}$$

was studied on the square domain [–0.5, 0.525] X [–0.5, 0.525].

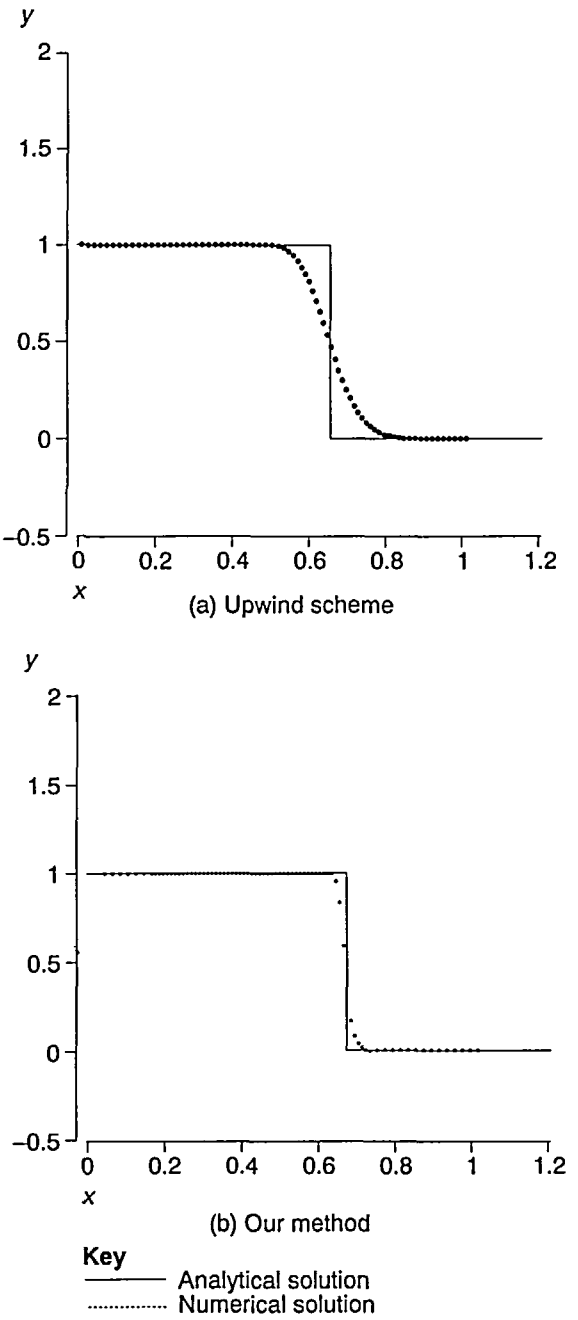

Figure 10 Equation (24)

The analytical solution of equation (28) is

$$\phi(x, y) = 0.09327 + (2.7E - 14) \exp(ux + vy). \tag{29}$$

In total, 289 volumes were defined with different sizes: a finer subdivision was defined where the gradient of the solution is high. The numerical solution with refinements and the analytical solution are represented in *Figure 12*.

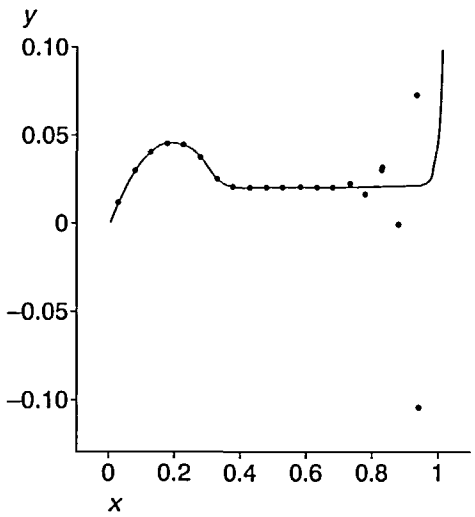

(a) Central scheme: $Pe = 5$

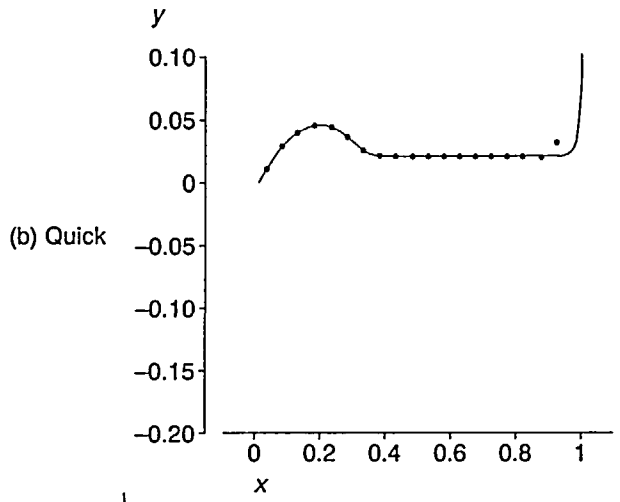

(b) Quick

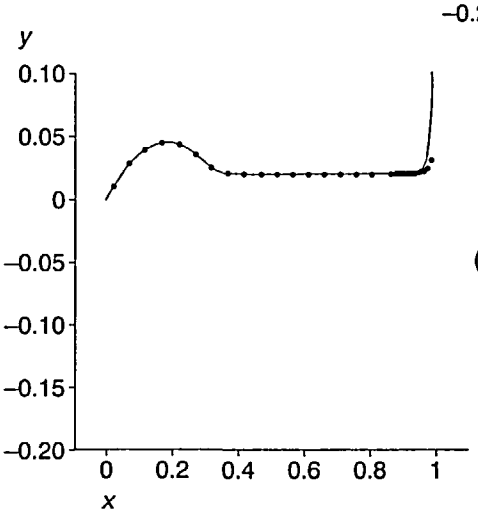

(c) Our method with unequal volumes

Figure 11 Solution of the 1D advection equation

Problem 2: the stationary equation proposed in Shih et al.[17]

$$u\frac{\partial\phi}{\partial x}+v\frac{\partial\phi}{\partial y}=\frac{\partial^2\phi}{\partial x^2}+\frac{\partial^2\phi}{\partial y^2}+S \tag{30}$$

where

$$S=-8\left(24y\,(x^4-2x^3+x^2)+(12x^2-12x+2)\,(4y^3-2y)\right)+ \tag{31}$$

$$-64\,(x^4-2x^3+x^2)\,(4x^3-6x^2+2x)\left((y^4-y^2)\,(12y^2-2)-(4y^3-2y)^2\right)$$

and the velocity components are:

$$u(x,y)=8\,(x^4-2x^3+x^2)\,(4y^3-2y) \tag{32}$$

$$v(x,y)=-8\,(4x^3-6x^2+2x)\,(y^4-y^2)$$

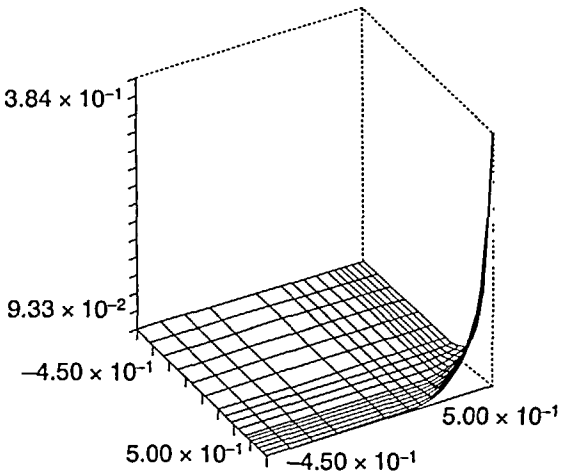

(a) Analytical

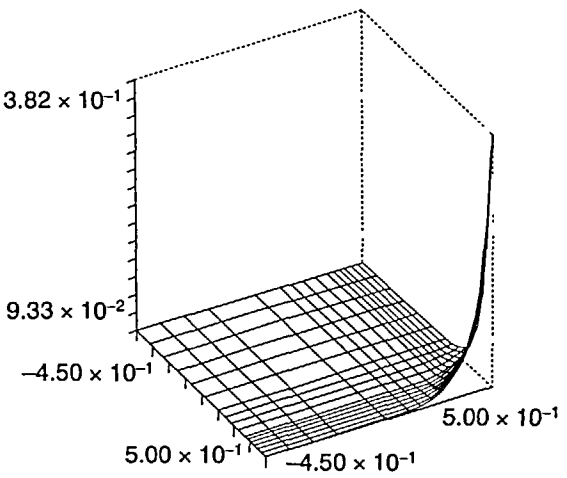

(b) Numerical

Figure 12 Solution of the 1D parabolic equation

The problem was solved on domain of *Figure 13*, subdivided in 88 volumes (neither equisized nor equishaped). The representation is on the unit square because of the graphical code.

The analytical and the numerical solutions are represented in *Figure 14* and the maximum error at internal volumes is $1.73E-3$, while at boundary volumes the maximum error is $5.1E-3$.

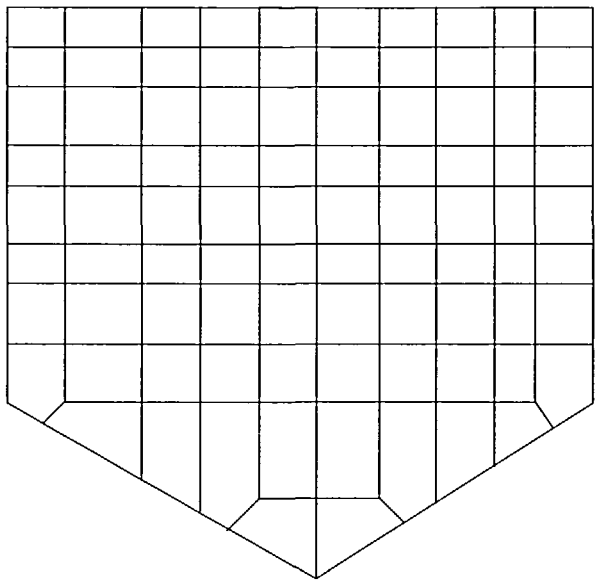

Figure 13 Domain for the solution of problem 2

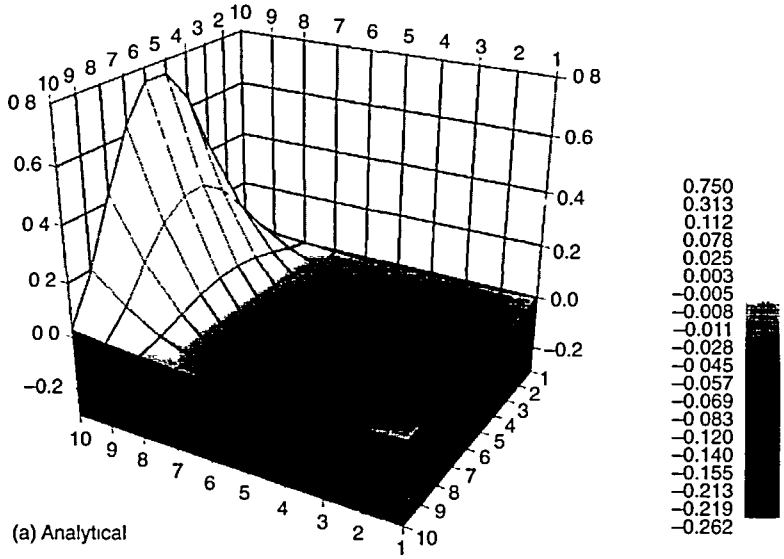

Figure 14 Solution of problem 2

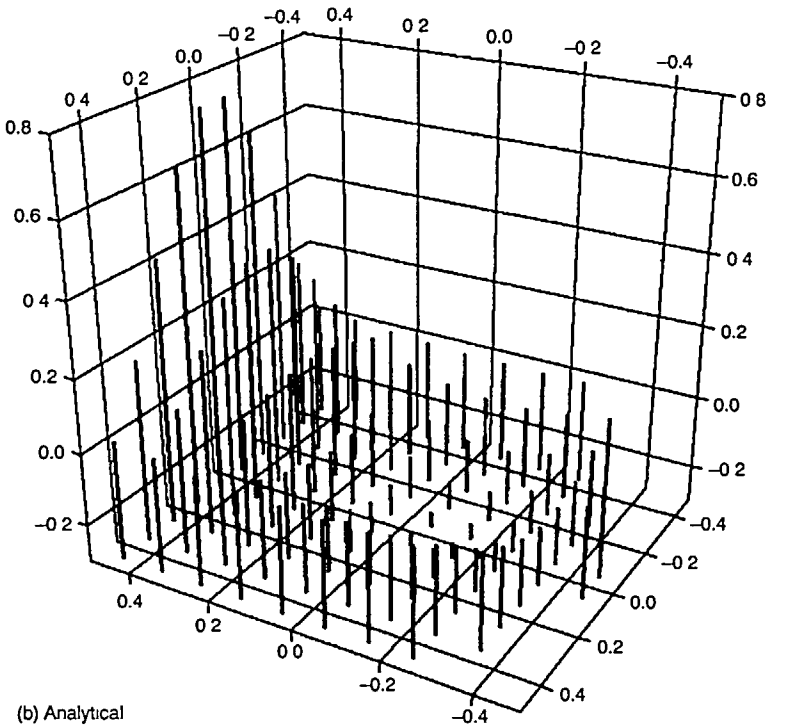

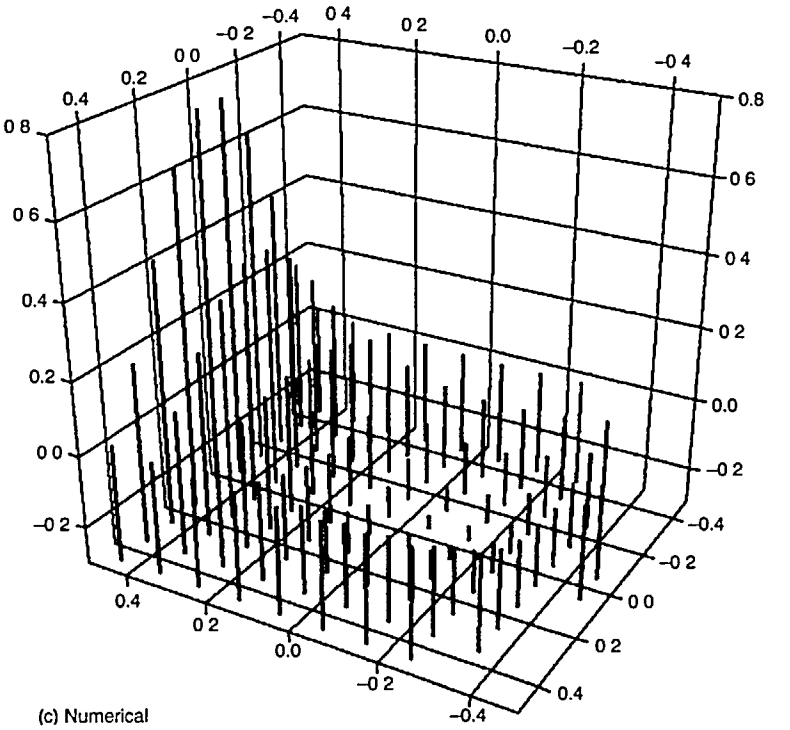

Figure 14 Continued

Problem 3: the unsteady equation proposed in Nguyen[18]

$$\frac{\partial \phi}{\partial t} + u\frac{\partial \phi}{\partial x} + v\frac{\partial \phi}{\partial y} - \Gamma\left(\frac{\partial^2 \phi}{\partial x^2} + \frac{\partial^2 \phi}{\partial y^2}\right) = 0 \tag{33}$$

was solved on the square $[-0.5, 0.5]\,X\,[-0.5, 0.5]$, with an explicit time advance technique.

The analytical solution is

$$\phi(x, y) = \frac{1}{\sigma(t)} \exp\left(-[(x - x_o - ut)^2 + (y - y_o - vt)^2]/(2\sigma^2(t)\right) \tag{34}$$

with $\sigma(t) = \sigma_o\,(1 + 2\Gamma t/\sigma_o{}^2)^{1/2}$, $\sigma_o = 0.0707$.

The domain was divided in 840 volumes. The analytical solution and the numerical solution are represented in *Figures 15, 16* and *17,* at time instants 0, 0.25, 0.5. The maximum errors were

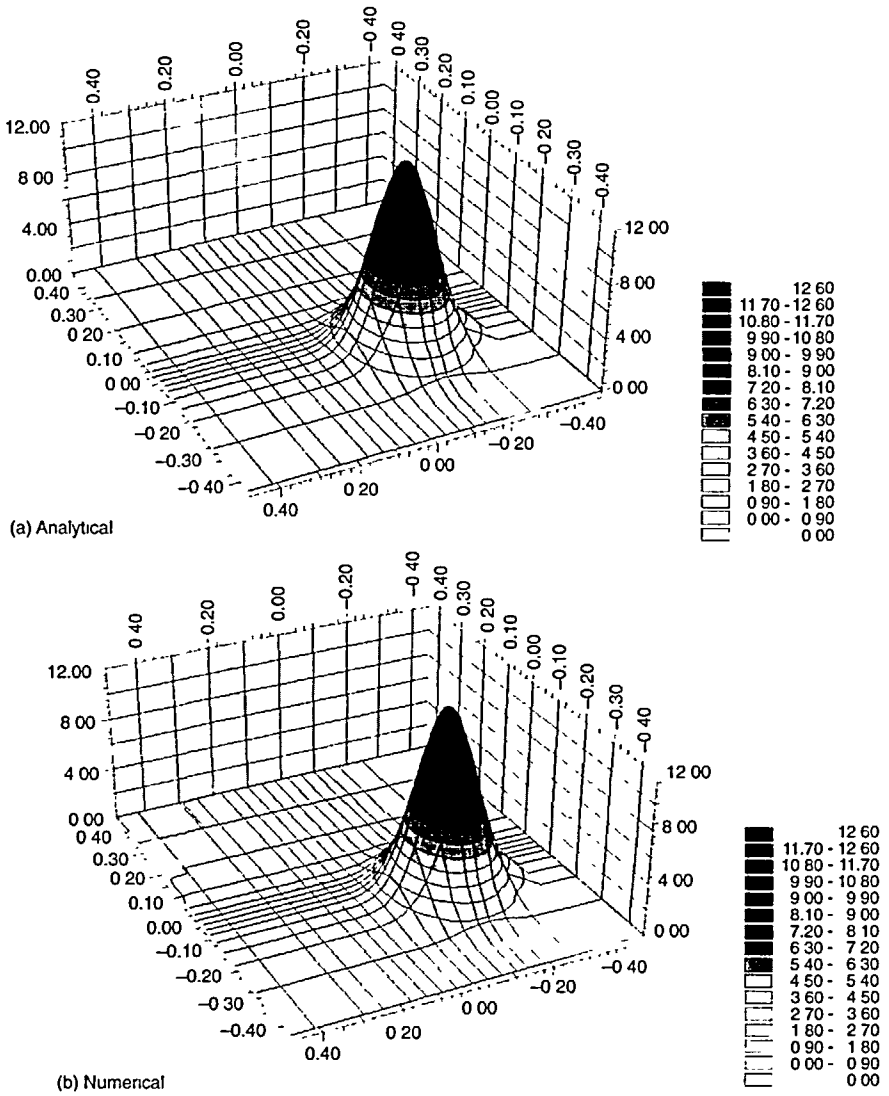

Figure 15 Solution of problem 3 after one time-step

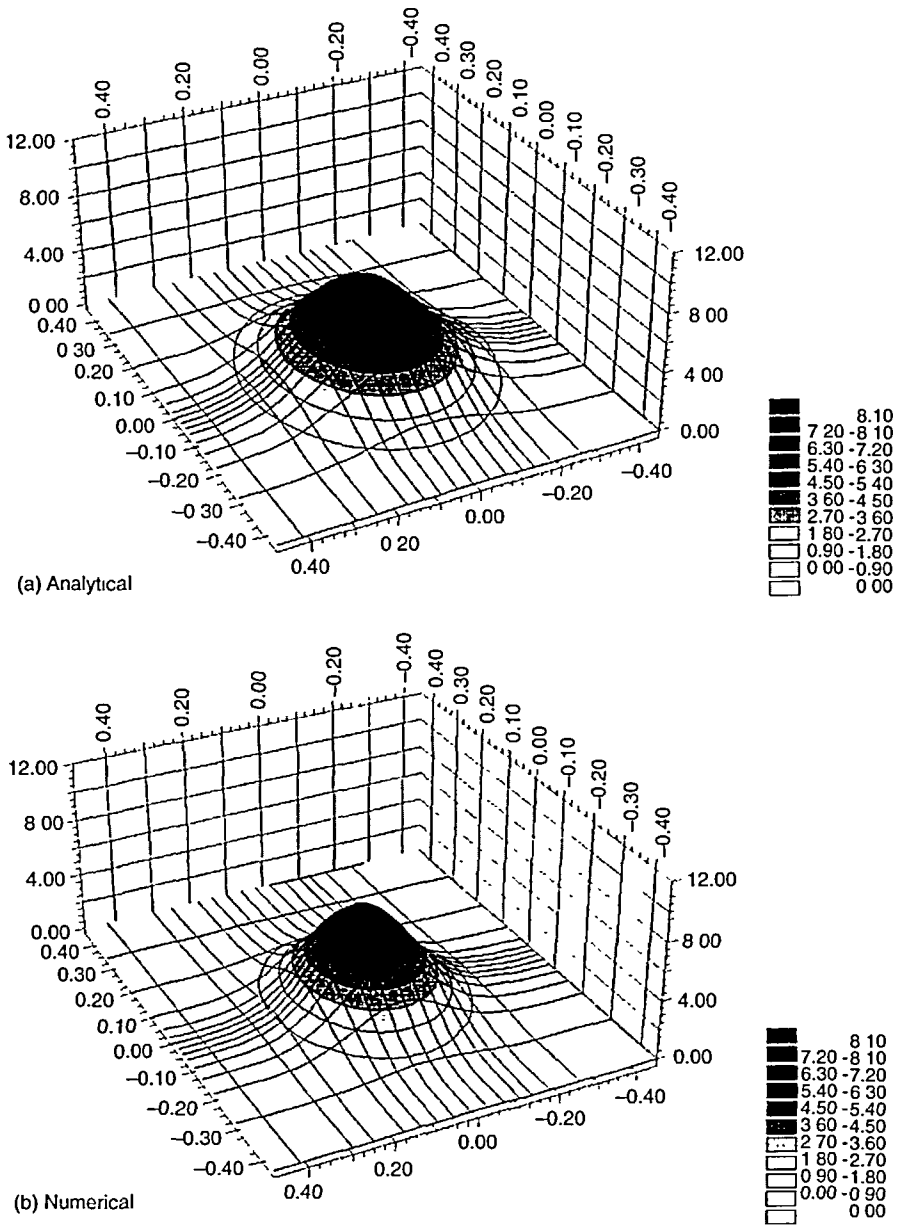

Figure 16 Solution of problem 3 at $t = 0.25$

$7.E-3$, $1.2E-1$ and $2.E-01$ respectively. To obtain this numerical solution we used the smoothing technique presented previously.

In order to compare our results to those presented in Nguyen[18], we also solved problem 3 on the unit square divided in 16 volumes and evaluated the error as in Nguyen[18]:

$$l_2 = \sum \frac{(\Phi_{num} - \Phi_{anal})^2}{\Phi_{anal}^2} \tag{35}$$

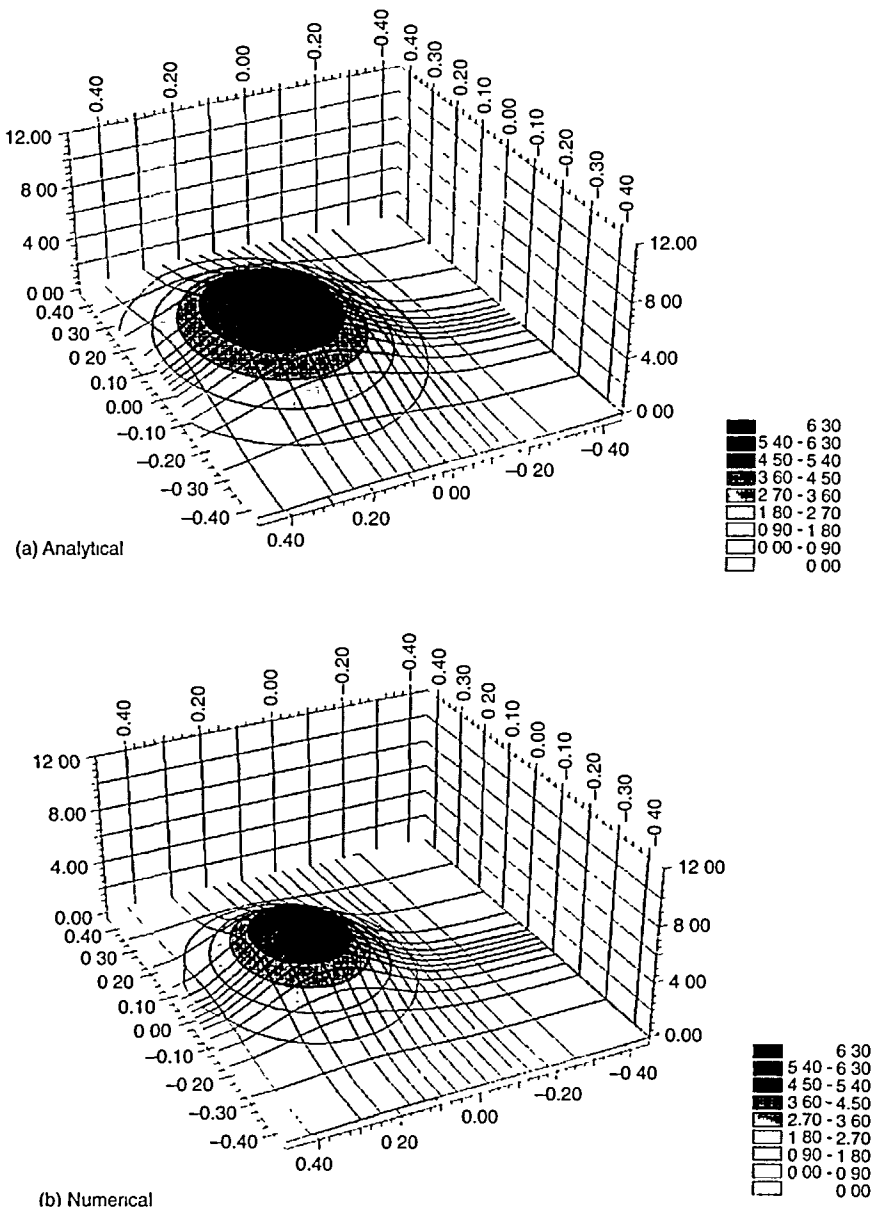

Figure 17 Solution of problem 3 at $t = 0.5$

We obtained errors of 0.31 for an explicit time advance technique, 0.29 for a Crank-Nicholson one and 0.36 for an implicit technique, while in Nguyen[18] the error is of 0.35 for a Petrov-Galerkin method with Crank-Nicholson technique.

CONCLUSION

In this paper a parabolic 1D profile which generalizes the well-known profile QUICK, by using not necessarily equisized volumes, has been presented.

A simple cubic non-linear 1D profile is used in the regions of high gradient to suppress spurious oscillations.

Finally, a 2D generalization has been proposed which, for not necessarily equisized or equishaped volumes, provides an effective numerical solution with a high order approximation of boundary conditions (even of Neumann type) on a polygonal approximation of the domain. By generalizing the 1D cubic profile, spurious oscillations are suppressed also in the 2D formulation.

The numerical results presented confirm the effectiveness of the refining technique. The method can easily be extended for the solution of scalar equations defined on 3D domains and has been used as a basis for the solution of Navier-Stokes problems defined on 2D domains[19,20].

ACKNOWLEDGEMENTS

This work was financially supported by ENEL SpA-CRIS. We are very grateful to the referees who reviewed this paper for their valuable suggestions.

REFERENCES

1 Pennati, V., Marelli, M. and De Biase, L., A generalized FV solution of convection-diffusion problems by means of monotonic v-splines profiles, submitted to *Heat and Fluid Flow*

2 Mackenzie, J.A. and Morton, K.W., Finite volume solutions of convection-diffusion test problems, *Math. of Comp.*, **60**, (201), 189-220, (1992)

3 *Handbook of Numerical Heat Transfer*, J. Wiley & Sons, New York (1988)

4 Thompson, J.F. *et al*, *Numerical Grid Generation: Foundations and Applications*, North Holland, Amsterdam (1985)

5 Leonard, B.P., A stable and accurate convective modelling procedure based on quadratic upstream interpolation, *Comput. Methods Appl. Mech. Engrg.*, **19**, 59-98, (1979)

6 Leonard, B.P., Simple high-accuracy resolution program for convective modelling of discontinuities, *Int. J. for Numer. Methods in Fluids*, **8**, 1291-1318 (1988)

7 Pennati, V., De Biase, L. and Feraudi, F., A generalized finite difference solution of parabolic 3D problems on multiconnected regions, *Comm. Appl. Num. Methods*, **8**, 361-371 (1992)

8 Casper, J. and Atkins, H.L., A finite-volume high-order ENO scheme for two-dimensional hyperbolic systems, *J. Comp. Physics*, **106**, 62-76 (1993)

9 Levy, D.W., Powell, K.G. and Van Leer, B., Use of a rotated Riemann solver for the 2D Euler equations, *J. Comp. Physics*, **106**, 201-214 (1993)

10 Rumsey, C.L., Van Leer, B. and Roe, P.L., A multidimensional flux function with applications to the Euler and Navier-Stokes equations, *J. Comp. Physics*, **106**, 201-214 (1993)

11 Leonard, B.P., The ULTIMATE conservative difference scheme applied to unsteady one-dimensional advection, *Comp. Meth. Appl. Mech. Eng*, **88** (1991)

12 Sweby, P.K., High resolution schemes using flux limiters for hyperbolic conservation laws, *SIAM J. Numer. Anal.*, **21**, 995-1011 (1984)

13 Leonard, B.P. and Mokhtari, S., Beyond first-order upwinding: the ULTRA-SHARP alternative for non-oscillatory steady-state simulation of convection, *Int. J. Numer. Methods Eng.*, **30**, 729-766 (1990)

14 De Biase, L., Feraudi, F. and Pennati, V., Temperature distribution in a polyedrical body with internal heat generation and flux boundary condition, *7th Int. Conf. on Num. Meth. in Thermal Problems*, Standford, July 1991

15 Whitham, G.B., *Linear and Nonlinear Waves*, J. Wiley & Sons, New York (1974)

16 Feraudi, F., Un nuovo metodo ai volumi finiti per la soluzione di problemi convettivo-diffusivi bidimensionali, PhD Thesis, University of Milano, 1994

17 Shih, T.M., Than, C.H. and Hwang, B.B., Effects of grid staggering on numerical schemes, *Int. J. for Num. Meth. in Fluids*, **9**, 193-212 (1989)

18 Nguyen, H., *Finite Elements Algorithms for the Simulation of Thermal Discharges into Coastal Waters of the Sea*, Commission of the European Communities Joint Research Centre, ISPRA-SITE, Progress Report, November 1992

19 Pennati, V., Feraudi, F., De Biase, L. and Valdani, S., A new finite volume method for the solution of 2D incompressible Navier-Stokes equations, *Numerical Methods in Laminar and Turbulent Flow, Vol IX*, Pineridge Press (1995)

20 De Biase, L., Feraudi, F. and Pennati, V., Solution of thermal benchmark problems by a new finite volume method, *Numerical Methods in Thermal Problems, Vol. IX*, Pineridge Press (1995)

FURTHER READING

Strickwerda, J.C., *Finite difference schemes and partial differential equations,* Wadsworth & Brooks/Cole Math. Series (1989).

APPENDIX

In this appendix we show, as an example of GFDF, the formulae we use for the approximation of the normal derivative at boundary point F of *Figure 6*. We write

$$\left.\frac{\partial u}{\partial n}\right|_F = \left.\frac{\partial u}{\partial x}\right|_F \cos\vartheta + \left.\frac{\partial u}{\partial y}\right|_F \cos\alpha$$

where α and ϑ are the angles between the normal direction and the co-ordinate axes x and y, respectively.

For a third order approximation of the normal derivative, we therefore need the partial derivatives to be of third order. We have:

$$\left.\frac{\partial u}{\partial x}\right|_F = -\frac{\nu+1}{2h(2+\nu)}u_{E1} + \frac{\nu+1}{2\nu h}u_{P1} - \frac{1}{\nu h(1+\nu)(2+\nu)}u_{P2} - \frac{1}{h(1+\nu)}u_F$$

or, by asymmetric stencil,

$$\left.\frac{\partial u}{\partial x}\right|_F = -\frac{2\nu^2+6\nu+3}{h(\nu+1)(2\nu+1)}u_F + \frac{(\nu+1)(2\nu+1)}{2h\nu^2}u_{P1} +$$

$$-\frac{2\nu+1}{h\nu^2(2\nu+1)}u_{P2} + \frac{\nu+1}{2h\nu^2(2\nu+1)}u_{P6}$$

For the partial derivative with respect to variable y at F the problem of missing information arises, since no grid points aligned with F are available.

Therefore a truncated Taylor expansion of the missing derivative is written:

$$\left.\frac{\partial u}{\partial y}\right|_F = \left.\frac{\partial u}{\partial y}\right|_{P1} + \left.\frac{\partial^2 u}{\partial x \partial y}\right|_{P1} h + \left.\frac{\partial^3 u}{\partial x^2 \partial y}\right|_{P1} h^2$$

where the partial derivatives in the formula above must be approximated to third, second and first order, respectively. Their approximations are:

$$\left.\frac{\partial u}{\partial y}\right|_{P1} = \frac{k_2(k_2+k_3)}{k_1(k_1+k_2+k_3)(k_1+k_2)}u_{P3} - \frac{k_1(k_2+k_3)}{k_2k_3(k_1+k_2)}u_{P4} +$$

$$+\frac{k_1k_2}{k_3(k_1+k_2+k_3)(k_2+k_3)}u_{P8} +$$

$$-\frac{(k_2+k_3)^2(-k_1^2-k_1k_3+k_2k_3)+k_1^2k_2^2}{k_1k_2k_3(k_1+k_2+k_3)(k_2+k_3)}u_{P1},$$

$$\left.\frac{\partial^2 u}{\partial x\,\partial y}\right|_{P1} = \frac{u_{P5}-u_{P2}-u_{P3}+u_{P1}}{\nu h k_1}.$$

For the third mixed derivative we give a more general formula, with respect to variables ξ and η, which, in turn will represent x and y. The points needed for the order of approximation required are in a greater number than in *Figure 6*. If, for example, we use a stencil as in *Figure A1*, the approximation for the third derivative is as follows:

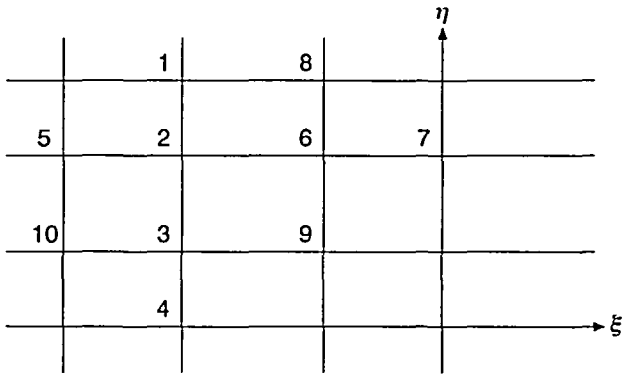

Figure A1

$$\left.\frac{\partial^3 u}{\partial \xi^2 \partial \eta}\right|_{P1} = \frac{1}{\eta_{10}(\xi_8 - \xi_9) + \eta_9(\xi_{10} - \xi_8) + \eta_8(\xi_9 - \xi_{10})}(mf + ng + pl)$$

where

$$m = \frac{2(\eta_8 - \eta_{10})}{(\eta_9 - \eta_2)(\xi_9 - \xi_2)};$$

$$f = u_9 - u_2 - (\eta_9 - \eta_2)\left.\frac{\partial u}{\partial \eta}\right|_2 - (\xi_9 - \xi_2)\left.\frac{\partial u}{\partial \xi}\right|_2 - \frac{1}{2}(\eta_9 - \eta_2)^2\left.\frac{\partial^2 u}{\partial \eta^2}\right|_2 +$$

$$-\frac{1}{2}(\xi_9 - \xi_2)^2\left.\frac{\partial^2 u}{\partial \xi^2}\right|_2 - \frac{1}{6}(\eta_9 - \eta_2)^3\left.\frac{\partial^3 u}{\partial \eta^3}\right|_2 - \frac{1}{6}(\xi_9 - \xi_2)^3\left.\frac{\partial^3 u}{\partial \xi^3}\right|_2$$

$$n = \frac{2(\eta_9 - \eta_8)}{(\eta_{10} - \eta_2)(\xi_{10} - \xi_2)}$$

$$g = u_{10}\,u_2 - (\eta_{10} - \eta_2)\left.\frac{\partial u}{\partial \eta}\right|_2 - (\xi_{10} - \xi_2)\left.\frac{\partial u}{\partial \xi}\right|_2 - \frac{1}{2}(\eta_{10} - \eta_2)^2\left.\frac{\partial^2 u}{\partial \eta^2}\right|_2 - \frac{1}{2}(\xi_{10} - \xi_2)^2\left.\frac{\partial^2 u}{\partial \xi^2}\right|_2$$

$$-\frac{1}{6}(\eta_{10} - \eta_2)^3\left.\frac{\partial^3 u}{\partial \eta^3}\right|_2 - \frac{1}{6}(\xi_{10} - \xi_2)^3\left.\frac{\partial^3 u}{\partial \xi^3}\right|_2$$

$$p = \frac{2(\eta_{10} - \eta_9)}{(\eta_8 - \eta_2)(\xi_8 - \xi_2)}$$

$$l = u_8 - u_2 - (\eta_8 - \eta_2)\left.\frac{\partial u}{\partial \eta}\right|_2 - (\xi_8 - \xi_2)\left.\frac{\partial u}{\partial \xi}\right|_2 - \frac{1}{2}(\eta_8 - \eta_2)^2\left.\frac{\partial^2 u}{\partial \eta^2}\right|_2 - \frac{1}{2}(\xi_8 - \xi_2)^2\left.\frac{\partial^2 u}{\partial \xi^2}\right|_2 +$$

$$-\frac{1}{6}(\eta_8 - \eta_2)^3\left.\frac{\partial^3 u}{\partial \eta^3}\right|_2 - \frac{1}{6}(\xi_8 - \xi_2)^3\left.\frac{\partial^3 u}{\partial \xi^3}\right|_2$$